MARM

Marmara Sea Reflection Profile

The Sea of Marmara – a 2-D Seismic Reflection Profile Data Archive

J.R. Parke, R.S. White, D. McKenzie
Bullard Labs, Madingley Road, Cambridge. CB3 0EZ, UK

T.A. Minshull, J. Bull
Southampton Oceanography Centre, Southampton. SO14 32H, UK

I. Kusçu
Maden Tetkik ve Arama Genel Müdürlügü, Ankara Turkey

N. Görür, A.M.C. Sengör
Istanbul Technical University, Maden Fakültesi, Jeoloji Bölümü, Ayazaga 80626, Istanbul Turkey

Data Set 03-001

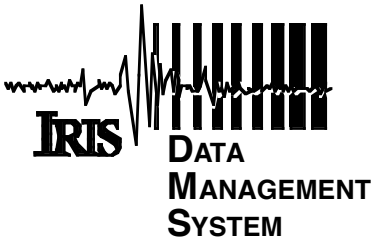

Distributed by:
Incorporated Research Institutions for Seismology
Data Management Center
1408 NE 45th Street, Suite 201
Seattle, Washington 98105 USA
www.iris.washington.edu

The Sea of Marmara - a 2D Seismic Reflection Profile Data Archive

J.R. Parke, R.S. White, D. McKenzie

Bullard Laboratories, Madingley Road, Cambridge. CB3 0EZ, UK

T.A. Minshull, J. Bull

Southampton Oceanography Centre, Southampton. SO14 32H, UK.

I. Kuşçu

Maden Tetkik ve Arama Genel Müdürlügü, Ankara, Turkey

N. Görür, A.M.C. Şengör

Istanbul Technical Üniversity, Maden Fakültesi, Jeoloji Bölümü, Ayazaga 80626, Istanbul, Turkey

Jeff Parke - parke@esc.cam.ac.uk 27 January 2003
Initally submitted to G-Cubed, 12 December 2002

Abstract

In 1997 1500 km of high resolution 2D reflection seismic data were acquired in the Sea of Marmara region, western Turkey. An archive of the 40 profiles of processed seismic data, in SEGY format, together with the DGPS (Differential Global Positioning System) locations and acquisition parameters for each profile are available for download from IRIS.

Introduction

The Marmara-97 multichannel seismic reflection profile data were collected between 29 August and 21 September 1997. This dataset has been used previously to generate a map of the faults in the Sea of Marmara [Parke, 1999,2002; Okay, 2000; Imren, 2000], but has not been presented in its entirety. Locations of the lines were planned based on a study of previous work [Barka, 1988; Wong, 1995; Smith, 1995] and of the known faults onshore, to the east, west and south of the Sea of Marmara [Saroglu, 1992] [Fig. 1]. The style of deformation onshore indicates a general east-west trend to the faults, which is borne out in the marine survey.

We recorded fewer profiles in the central part of the northern Sea of Marmara, due to the logistic constraints of major shipping lanes in this area, and to time constraints for the survey. The east-west tie lines were for the most part over the southern shelf, leading to difficulties in correlating the stratigraphy in the deep basins, although penetration was not sufficiently deep to be able to image the basement reflectors in these areas anyway.

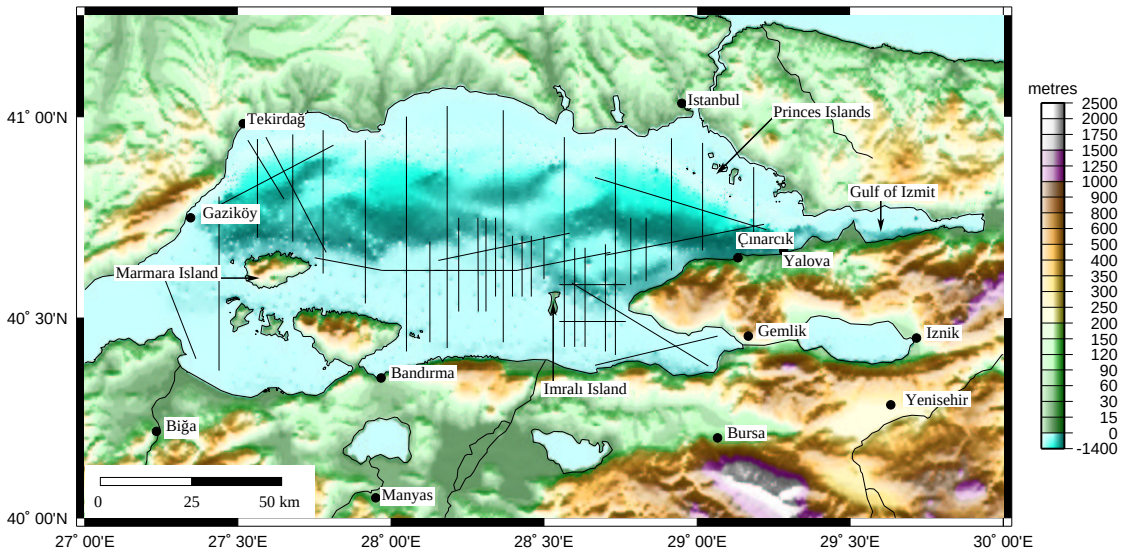

Figure 1: Map of the Sea of Marmara region, showing the locations of the seismic reflection profiles acquired in 1997 (solid lines), and the Turkish Petroleum profiles available prior to acquisition (dashed lines). Topography is from the USGS GTOPO30 dataset. Bathymetry has been digitised from Turkish Admiralty maps.

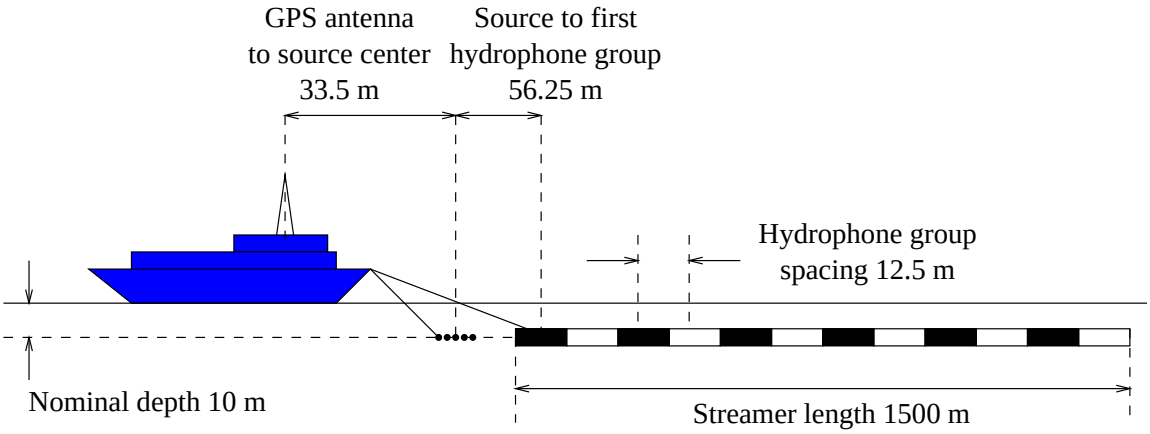

Figure 2: Schematic diagram of ship geometry during Marmara Sea cruise. All distances are measured in meters relative to the GPS antenna on the ship. The configuration shown is for a maximum streamer length of 1,500 m.

Data Acquisition

The normal-incidence multichannel seismic data acquired during the Marmara-97 cruise were recorded using a 120 channel streamer with a 12.5 m group interval; a total length of 1500 m [Fig. 2]. During acquisition, some sections of the streamer proved unreliable, so the number of active channels varied from 66 to 120, with a corresponding variation of fold in the data.

Each airgun in the 10-gun array had a selectable capacity of either 90 in^3 or 210 in^3. A larger shot spacing would therefore allow more time for the compressor to resupply the array, and hence allow a larger array volume. An optimal volume of 1380 in^3 was used (4 airguns at 210 in^3 and 6 at 90 in^3) which was triggered every 50 m, shooting on distance, from differential GPS (DGPS), or at fixed time intervals of 22 seconds, when DGPS was unavailable (<1% of acquisition).

The streamer was equipped with 10 'birds' to assist depth control when towing. The bird wings had a pitch variation of $\pm 17^o$ from the horizontal and were used to attain a nominal streamer depth of 10 m. This depth varied considerably due to

variations in speed of the ship, largely because of other traffic. The changes in speed caused the streamer to kink and bow in the water, and this is manifested by some noisier parts of the data. The birds also had electronic compasses, which gave an indication of their heading. The acquisition system logged the location of the ship, water depth, bird depth and heading for each shot.

From examination of the magnetic data from the birds, the streamer was at times being towed at an angle of 20^{o} to the sail line. This leads to an off-line location of $\sim$600 m at the far end of the streamer, and the tail-buoy. This does not appear to be significant in deeper water, but means that far-offset arrivals at the start and end of the lines, when the streamer may not be straight, are very different from near-offset. This problem is most apparent in shallow water. It was overcome by applying a time-offset dependent mute to the shot gathers. This removed refracted arrivals at far-offsets in shallower water, and spurious arrivals at the start and end of the lines when the ship was turning in a tight arc.

Processing

The processing scheme [Fig. 3] began with the SEG-Y data being read in from field tapes, during which the data were resampled to 4 ms, and record length 5 s. Every 30th shot (roughly 10 minutes of acquisition) was examined visually for dead or noisy channels, which were then muted.

The data were then bandpass filtered with an Ormsby minimum phase bypass gate filter [Yilmaz, 1987] at 3-5-80-120 Hz and sorted into their CDP bins, with a t-squared amplitude recovery gain [Fig. 3].

For brute processing of the reflection data, the following strategy was devised: the near-offset channel (96) was displayed, and the sea-floor two-way time (TWT) was picked. An interval velocity model was generated, with velocities of 1500 m/s, 1800

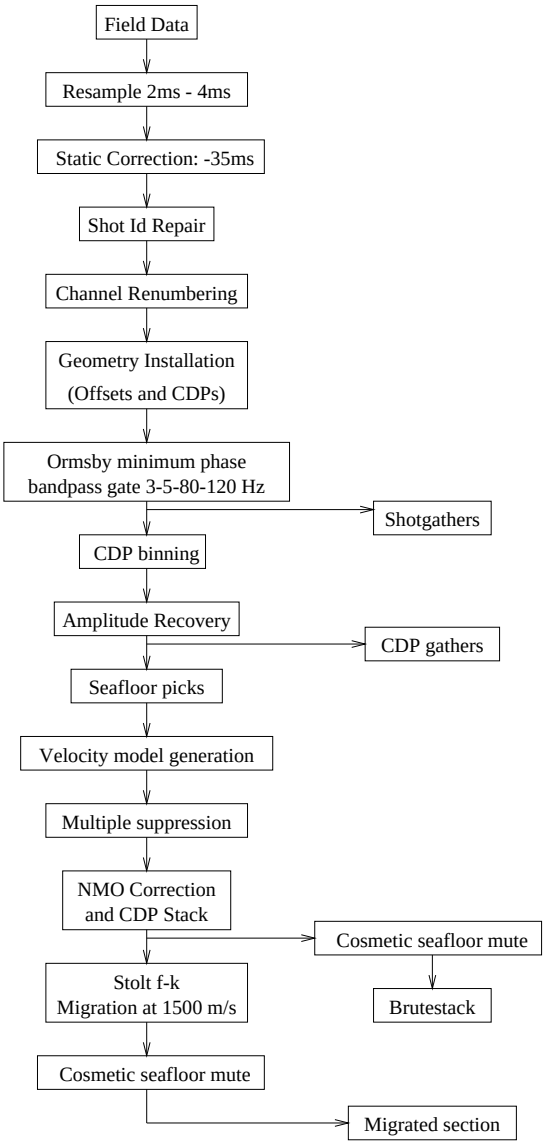

Figure 3: Flow diagram showing the generic processing steps applied to the seismic data during reprocessing.

m/s, 2500 m/s and 4000 m/s at 0 ms, 500 ms, 1500 ms and 2500 ms below the seafloor respectively. These numbers were based on velocity analyses of the first few lines acquired, and were generally a good basis for the velocity structure of the basin fill sediments elsewhere in the area. This model was converted to RMS velocities, and applied as a normal moveout correction to the data, with a 30% stretch mute. The data

were mean trace summed, normalised by $\sqrt{n}$.

During reprocessing of specific sections of the reflection profile data, an RMS velocity function was determined by normal moveout (NMO) velocity analysis using constant velocity NMO corrected CDP gathers and semblance analysis plots [Yilmaz, 1987]. The volume of data acquired was too great to permit a high resolution analysis everywhere, so a generic strategy was devised in which velocities were picked approximately every 2000 CDPs, or where there was a visible change in lithology in the brute stacked profile. Where sections were processed to highlight a particular feature, a specific velocity model was picked for that area.

The data were next muted with a linear ramp from maximum at 4500 ms down to zero amplitude at 5000 ms. Stolt *f-k* migration [Stolt, 1978] was performed with a uniform water velocity of 1500 m/s. A cosmetic sea-floor mute was applied to both the stack and the migration before printing for interpretation.

Reflection Profile Data

For the purposes of this distribution, the CDP bin spacing has been doubled from 6.25 m to 12.5 m, in order to reduce the size of the dataset. This doubling was achieved by binning consecutive pairs of traces in the stacked data. Consequently only the odd CDP numbers are present in the stacked and migrated profiles presented here. The high frequency of the source wavelet means that the data are useful for observing small features associated with shelf processes [*e.g.* Fig. 4]. The dataset coverage of the Sea of Marmara also means that regional basin spanning lines are available [Fig. 5]

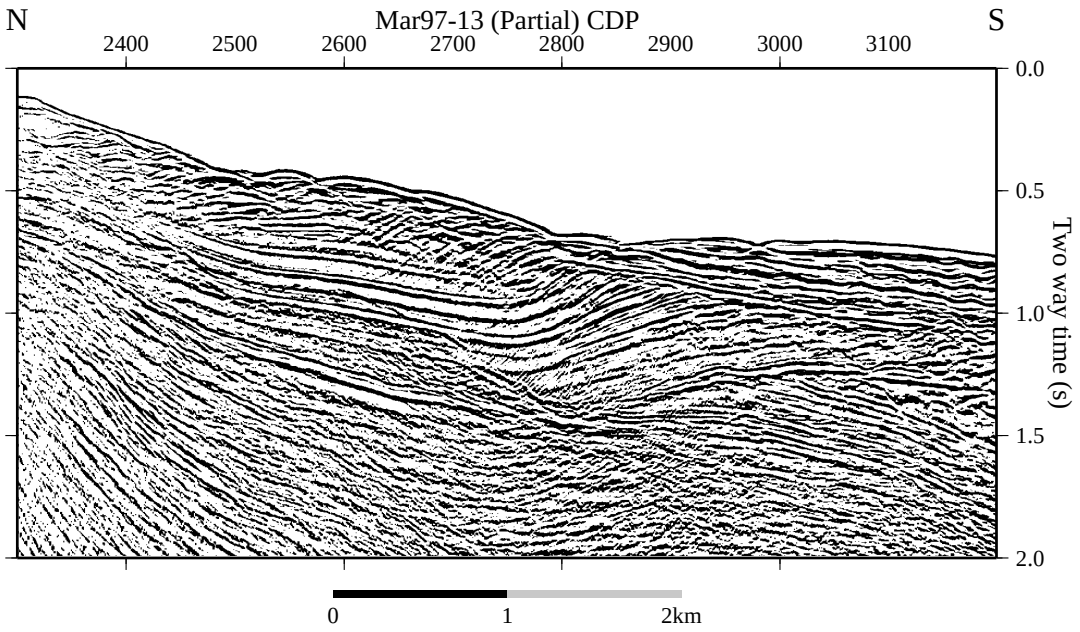

Figure 4: Sample migrated reflection profile from the central Sea of Marmara, showing unconformities in the shelf sediments.

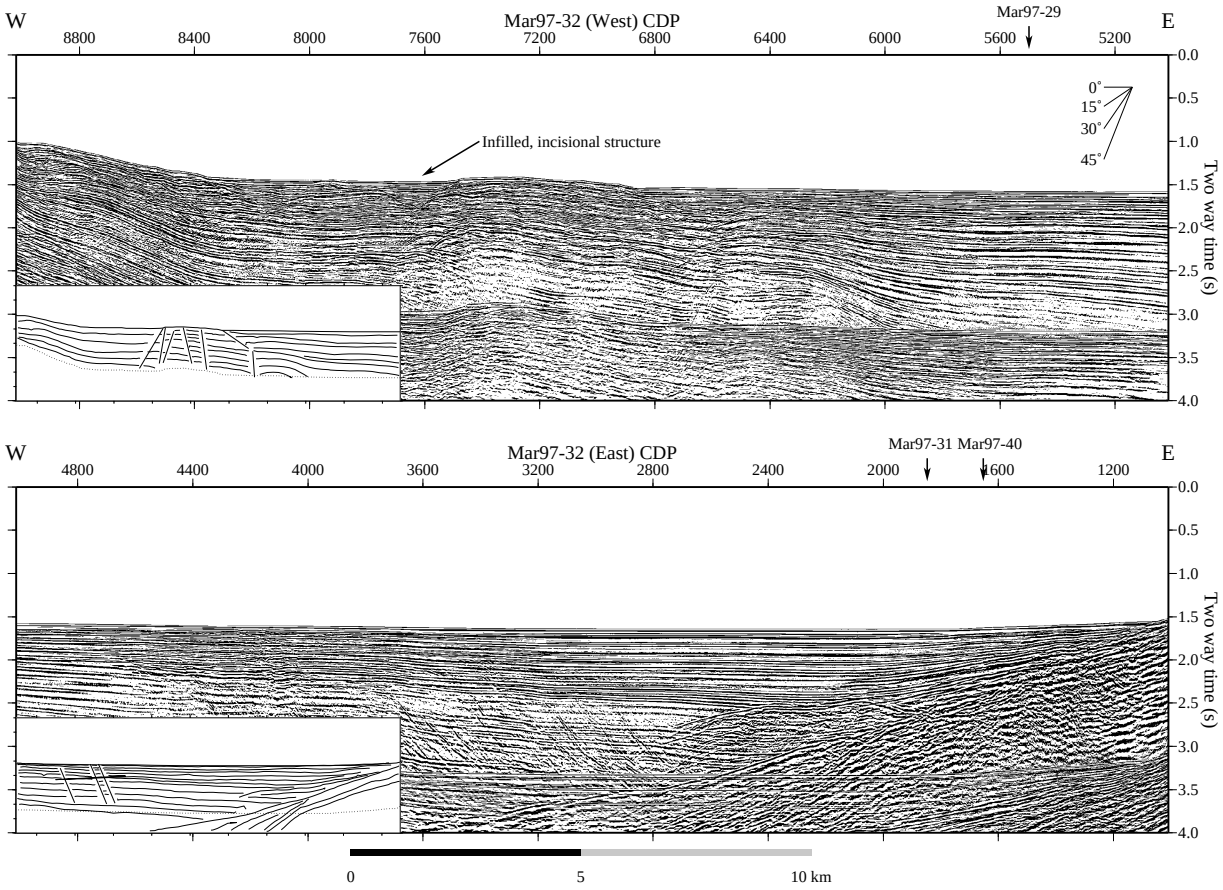

Figure 5: Sample migrated reflection profile from the eastern Sea of Marmara, showing dipping limestone basement from CDP 1000-3600, with unconformable deposits above. An infilled incisional canyon is highlighted at CDP 7600.

The data archive also includes the acquisition parameters for each profile, as well as the differential GPS shot locations, and locations of the CDP bins for each line. The complete dataset is available for download from IRIS. Users who wish to request the dataset should go to:

http://www.iris.washington.edu/data/req_methods.htm

From there, one should select the 'Assembled Set web form' tool. The Assembled Set title for this dataset is 'Marmara Sea Reflection Profile' (nickname MARM). The dataset number is 03-001.

Acknowledgements

We thank the captain, officers, crew, and scientific party of the R/V MTA Sismik 1, for their assistance during the Marmara cruise in September 1997, and the Royal Society for funding this research. Earth Sciences contribution number 6628 [University of Cambridge].

References

Barka, A. & Kadinsky-Cade, K. Strike-slip fault geometry in Turkey and its influence on earthquake activity. *Tectonics*, **7**, 663–684, 1988.

İmren, C., Le Pichon, X., Rangin, C., Demirbağ, E., Ecevitoğlu, B. & Görür, N., The North Anatolian Fault within the Sea of Marmara: A new evaluation based on multichannel seismic and multibeam data. In *American Geophysical Union, Fall Meeting Abstracts*, F1222 (2000).

Okay, A., Kaşlılar-Özcan, A., İmren, C., Boztepe-Güney, A., Demirbağ, E. & Kuşçu, İ. Active faults end evolving strike-slip basins in the Marmara Sea, northwest

Turkey: a multichannel seismic reflection study. *Tectonophysics*, **321**, 189–218, 2000.

Parke, J.R., Minshull, T.A., Anderson, G., White, R.S., M^{c}Kenzie, D., Kuscu, I., Bull, J., Gorur, N. & Sengor, A.M.C. Active faults in the Sea of Marmara, western Turkey, imaged by seismic reflection profiles. *Terra Nova*, **11**, 223–227, 1999.

Parke, J.R., Minshull, T.A., Anderson, G., White, R.S., M^{c}Kenzie, D., Kuscu, I., Bull, J., Gorur, N. & Sengor, A.M.C. Interaction between faulting and sedimentation in the Sea of Marmara, western Turkey. *Journal of Geophysical Research*, **107**, 2286–2305, 2002.

Şaroglu, F., Emer, O. & Kuşçu, I. Active fault map of Turkey. *General Directorate of Mineral Research and Exploration, Ankara*, 1992.

Smith, A., Taymaz, T., Oktay, F., Yüce, H., Alpar, B., Başaran, H., Jackson, J., Kara, S. & Şimşek, M. High-resolution seismic profiling in the Sea of Marmara (north-west Turkey): Late Quaternary sedimentation and sea-level changes. *Geological Society of America, Bulletin*, **107**, 923–936, 1995.

Stolt, R. Migration by Fourier transform. *Geophysics*, **43**, 23–48, 1978.

Wong, H., Lüdmann, T., Ulug, A. & Görür, N. The Sea of Marmara: A plate boundary sea in an escape tectonic regime. *Tectonophysics*, **244**, 231–250, 1995.

Yilmaz, Ö., *Seismic Data Processing* (Society of Exploration Geophysicists, 1987).